An experimental assessment of analytical blockage corrections for turbines

Hannah Ross*, Brian Polagye

Department of Mechanical Engineering, University of Washington, Seattle, WA 98195, USA

Abstract

In laboratory experiments involving wind or water turbines, it is often desirable to correct measured performance for the effects of model blockage. However, there has been limited experimental validation of the analytical blockage corrections presented in the literature. Therefore, the objective of this study is to evaluate corrections against experimental data and recommend one or more for future use. For this investigation, we tested a cross-flow turbine and an axial-flow turbine under conditions of varying blockage with other non-dimensional parameters, such as the free-stream Reynolds and Froude numbers, held approximately constant. We used the resulting experimental data to assess the effectiveness of multiple analytical blockage corrections for both turbine types. Of the corrections evaluated, two are recommended. However, as these methods are based on axial momentum theory, we observe that corrections are more effective for thrust than power. We also find that increasing blockage changes the local Reynolds number, which can affect turbine performance but is not reflected in axial momentum theory.

Keywords: flow confinement, blockage corrections, tidal energy, wind energy

1. Introduction

Naturally occurring fluid flows, such as wind and water currents, are a promising source of renewable power. The turbines that convert energy from these currents into electricity can operate in confined flows, such as rivers and tidal channels, and experimental investigations of scale models often take place in confined wind or water tunnels. Flow confinement, or blockage, can significantly alter the mechanical performance of a turbine, relative to operation in an unconfined flow. The effects of blockage on propeller aero-

*Corresponding author.
Email address: hkross@uw.edu (Hannah Ross)

dynamics were examined in the early 20th century by Wood and Harris [1] and Glauert [2]. More recently, analytical [3, 4], numerical [5–11], and experimental [12–18] studies have explored the effects of blockage on wind and water current turbines. The magnitude of these effects is related to the blockage ratio (β), a dimensionless quantity defined as $\beta = (A_T + A_S)/A_C$, where A_T is the projected area of the turbine rotor, A_S is the projected area of the support structure, and A_C is the cross-sectional area of the channel. Multiple studies have demonstrated that turbine performance changes appreciably when the blockage ratio exceeds 5-10% [8, 10, 15, 18]. Turbine performance can be described by the cycle-average power and thrust coefficients (C_P, C_T) over a range of tip-speed ratios (λ),

$$C_P = \frac{\langle \tau\omega \rangle}{\frac{1}{2}\rho A_T \langle V_0^3 \rangle}, \tag{1}$$

$$C_T = \frac{\langle T \rangle}{\frac{1}{2}\rho A_T \langle V_0^2 \rangle}, \tag{2}$$

$$\lambda = \frac{R\langle \omega \rangle}{\langle V_0 \rangle}, \tag{3}$$

where τ is the measured torque, ω is the angular velocity of the turbine, ρ is the fluid density, V_0 is the free-stream velocity, T is the thrust on the turbine, and R is the rotor radius. Note that $P = \tau\omega$, where P is the mechanical power produced by the turbine. For a turbine operating at a given tip-speed ratio, higher blockage increases stream-wise flow speeds through and around the rotor [6, 8, 11, 15]. These higher velocities at the rotor plane increase the turbine's torque and thrust. However, the flow velocity far upstream of the turbine remains relatively unchanged. Therefore, increasing the blockage augments a turbine's power and thrust coefficients for a given free-stream velocity and tip-speed ratio. More detailed discussions about the effects of blockage on turbine hydrodynamics are given by Houlsby and Vogel [4] and Consul et al. [6].

Research on blockage effects has two primary motivations. First, turbine testing is often conducted in laboratory facilities, such as wind and water tunnels, or in numerical simulations with finite domains. To accurately model full-scale conditions, the influence of blockage on performance data collected at smaller scales must be accounted for. Second, the observation that blockage can augment turbine performance has inspired interest in the design of high-blockage "fences" of current turbines [9], which would operate in flows that are naturally constrained, such as rivers and tidal channels. A better understanding of blockage could enable more accurate predictions of the power output from such arrangements.

Over the past century, analytical methods have been developed to account for blockage effects. These methods are often referred to as "blockage corrections" and are the focus of this study. The first such correction was developed by Glauert [2] for propellers tested in wind tunnels. Glauert's method is based on axial momentum theory applied to an actuator disc (i.e., linear momentum actuator disc theory) in a closed tunnel. The most common form of this correction is an approximation based on the assumption that the blockage ratio is less than 0.15. Glauert's approximate correction can be applied to turbines, but it has a limited range of applicability due to a singularity as the thrust coefficient approaches unity [13]. Subsequent studies, following Glauert's approach, have derived corrections specifically for wind and current turbines. Here, we focus on the corrections presented by Barnsley and Wellicome [19], Mikkelsen and Sørensen [20], Werle [21], and Houlsby et al. [22]. All are derived from axial momentum theory applied to an actuator disc in a flow confined either by rigid walls (e.g., a tunnel) or by rigid walls and a free surface (e.g., a channel). These corrections have seen widespread application to performance data from experiments and simulations [8, 12, 15, 16, 23]. However, uncertainty remains as to which corrections, if any, effectively account for blockage [11, 23, 24].

Several previous studies have attempted to address the question of correction efficacy. Kinsey and Dumas [11] simulated a cross-flow turbine (i.e., "vertical-axis", where the axis of rotation is perpendicular to the flow direction) and an axial-flow turbine (i.e., "horizontal-axis", where the axis of rotation is parallel to the flow direction) operating in a water tunnel and applied the correction of Barnsley and Wellicome [19]. By comparing the corrected results to simulations conducted in an unconfined domain, they concluded that Barnsley and Wellicome's method worked well for the axial-flow turbine and was adequate for the cross-flow turbine. Similarly, Segalini and Inghels [25] simulated blockage effects on an axial-flow turbine using a vortex model and compared power and thrust corrections estimated from this model to those given by the actuator disc method of Mikkelsen and Sørensen [20]. Results from the two methods agreed reasonably well, providing encouraging validation of actuator disc corrections applied to realistic turbines. Experimentally, Ryi et al. [17] applied Barnsley and Wellicome's correction to an axial-flow turbine tested in a closed-section wind tunnel and found that corrected results agreed well with the same turbine's performance in an open-jet wind tunnel. Using similar methods, Dossena et al. [18] conducted experimental wind tunnel tests of a cross-flow turbine at a blockage ratio of 10% and under conditions of negligible blockage. They compared an empirical correction based on experimental data from the two conditions with an analytical correction using Mikkelsen and Sørensen's method. They concluded that the analytical method predicted the trend of the empirical correction but significantly underestimated its magnitude. The authors recommended improving analytical blockage corrections specifically for cross-flow turbines.

Several recent studies [11, 13, 26–28] have also examined the effectiveness of blockage corrections originally derived for bluff bodies [29, 30], when applied to turbines. For example, Whelan et al. [26] and Kinsey and Dumas [11] determined that Maskell's correction performs better than actuator disc methods when the turbine rotor is heavily loaded.

Overall, previous research has concluded that actuator disc corrections are adequate for axial-flow turbines and give mixed results for cross-flow turbines. However, prior studies have evaluated only one or two of the multiple blockage corrections proposed in the literature. Because the effectiveness of a blockage correction depends on the specific conditions under which it is applied (e.g., turbine and support structure design and tunnel or channel geometry), the relative accuracy of these corrections remains an open question. To our knowledge, no systematic experimental validation that considers both turbine archetypes and multiple analytical corrections has been reported in the archival literature. This lack of validation may be a consequence of the difficulty of undertaking such experiments, which require varying blockage while controlling for Reynolds number dependence [31–33] and, in the case of a free surface, the Froude number and submergence depth [8, 34]. For experiments conducted at transitional Reynolds numbers, this can only be achieved by changing the physical dimensions of a tunnel or the width of a channel. Therefore, the objective of the present study is to experimentally evaluate blockage corrections for a cross-flow and an axial-flow turbine by varying the blockage ratio while other significant parameters are held approximately constant.

2. Experimental methods

To establish a baseline for the analytical corrections, a cross-flow and an axial-flow turbine were characterized under high blockage and negligible blockage by testing the turbines at experimental facilities of different size. The subsequent sections describe the turbines, facilities, experimental parameters, and methods of data acquisition and analysis.

2.1. Turbines

The cross-flow turbine has four straight blades capped by circular end-plates. The turbine has a diameter (D) of 0.51 m and a height of 0.31 m. The aluminum blades are NACA-0018 airfoils, each with a chord length of 0.06 m, mounted with a neutral preset pitch. Two six-axis load cells, attached above and below the turbine, were used to measure the forces and torque. The angular velocity of the turbine was controlled by a servomotor, and a rotary encoder was used to measure the turbine's angular position. An acoustic Doppler velocimeter measured the free-stream velocity at the turbine mid-plane at a distance of 5 diameters upstream from the axis of rotation. A schematic of the experimental set-up is given in Fig. 1(a), and additional details about the data acquisition system are given by Strom et al. [35].

The axial-flow turbine has three variable-pitch NACA-44xx aluminum blades, a rotor diameter of 0.45 m, and a hub diameter of 0.11 m. For this study, the blades were fixed at

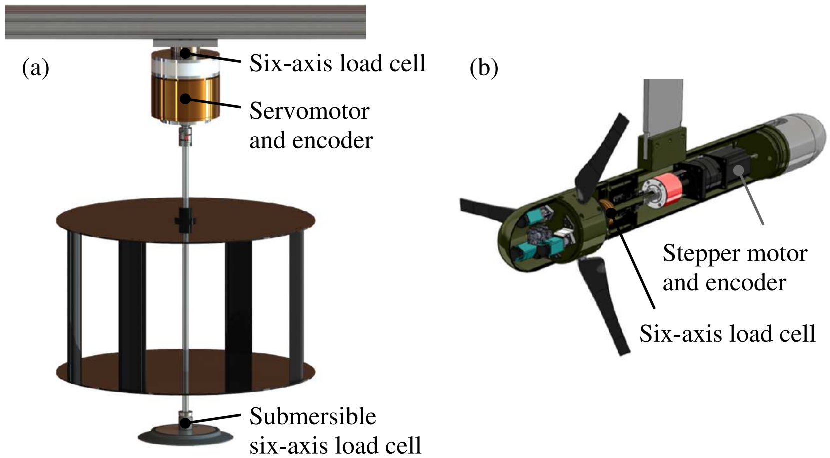

Fig. 1. Renderings of the cross-flow (a) and axial-flow (b) experimental turbines used in this study.

a pitch angle of 0°. A six-axis load cell mounted between the drive shaft and hub was used to measure the forces and torque. The speed of the rotor was regulated by a stepper motor, and the rotor position was measured with an optical encoder. The free-stream velocity was measured with an acoustic Doppler velocimeter located 3 diameters upstream of the rotor plane. Fig. 1(*b*) shows a schematic of the turbine, and further information about the blade geometry and instrumentation is given by Barber et al. [36].

2.2. Testing facilities

To achieve conditions of high and negligible blockage, the turbines were tested in two facilities: the Alice C. Tyler flume in the Harris Hydraulics Laboratory at the University of Washington (UW) and the tow tank at the Jere A. Chase Ocean Engineering Laboratory at the University of New Hampshire (UNH). The UW flume is a high blockage environment consisting of a rectangular test section that is 0.76 m wide, 0.60 m deep, and 3.7 m long. Two variable-frequency pumps operating in parallel can achieve a maximum flow speed of 1.2 m/s. A pool heater and chiller enable the water temperature to be controlled between 10 and 35°C. The turbulence intensity is approximately 2% under most operating conditions. The UNH tow tank is a negligible blockage environment roughly 3.7 m wide, 2.4 m deep, and 36 m long. The turbulence intensity is approximately 0%, and the water is room temperature, between 20 and 22°C. Additional information about the UNH facility is given by Bachant and Wosnik [37].

As detailed, there was a small difference in turbulence intensity between the two facilities. Past studies have shown that decreasing the turbulence intensity increases a turbine's power and thrust coefficients [38, 39]. However, based on the magnitude of performance change observed in these studies, it is assumed that the impact of a decrease in turbulence intensity from approximately 2% to approximately 0% is insignificant.

2.3. Non-dimensional parameters

The dimensions of the UW flume resulted in a blockage ratio of 0.36 for the cross-flow turbine and 0.35 for the axial-flow turbine. The larger cross-section of the UNH facility yielded a blockage ratio of 0.03 for the cross-flow turbine and 0.02 for the axial-flow turbine. Consequently, the blockage effects at the UNH facility were assumed to be negligible [10]. We will refer to data taken in the UW flume as "confined" and data taken in the UNH tow tank as "unconfined". To measure only the effects of a change in blockage, we attempted to hold all other important parameters approximately constant: the chord-based Reynolds number, $Re_c = (cV_0)/\nu$, the Froude number, $Fr = V_0/\sqrt{gd_0}$, and the submergence depth, d_T, measured from the free surface to the top of the rotor. Here, c is the blade chord length, ν is the fluid kinematic viscosity, g is the acceleration of gravity, and d_0 is the undisturbed upstream water depth, relative to the bottom of the channel. Under test conditions, both turbines were operating at transitional Reynolds numbers: 31 000 for the cross-flow turbine and 14 000 for the axial-flow turbine. To maintain a constant Reynolds number, all tests were conducted at a free-stream velocity of 0.5 m/s and, because viscosity is a function of temperature, the UW flume was controlled to match the temperature of the UNH tow tank. In the UW flume, the turbines were centered horizontally between the channel walls and vertically in the dynamic water column. This resulted in a submergence depth of 0.15 m for the cross-flow turbine and 0.08 m for the axial-flow turbine. Both turbines were mounted in the tow tank such that submergence depth remained constant between the two facilities. However, the variation in overall channel depth from 0.60 m in the flume to 2.4 m in the tow tank resulted in a change in the Froude number from 0.2 to 0.1. Given that no free surface deformation was observed at either facility, it was assumed that this variation in Froude number had a negligible effect on performance compared to the changes in blockage [6].

Although both turbines were centered in the UW flume, the aspect ratio of the channel resulted in higher horizontal blockage for the cross-flow turbine and higher vertical blockage for the axial-flow turbine. Kinsey and Dumas [11] defined the confinement asymmetry as $CA = \max(\beta_H/\beta_V, \beta_V/\beta_H)$, where β_H is the ratio of turbine width to channel width and β_V is the ratio of turbine height to fluid depth. The authors concluded that a confinement asymmetry that exceeds unity does affect performance, relative to a turbine operating with symmetric confinement at the same blockage ratio. However, they also found that confinement asymmetry is negligible for $CA < 3$. As the confinement asymmetry of both turbines in the UW flume was approximately 1.3, we assume performance was relatively unaffected by the channel aspect ratio.

2.4. Performance characterization

At each nominal operating condition (i.e., tip-speed ratio), performance data were collected for at least 30 seconds. The time series were trimmed to yield an integer number of rotor revolutions. To calculate C_P, C_T, and λ according to Eqs. (1)-(3), the quantities $\langle \tau\omega \rangle$, $\langle T \rangle$, and $\langle \omega \rangle$ were averaged over each complete revolution of the turbine rotor, and $\langle V_0^3 \rangle$, $\langle V_0^2 \rangle$, and $\langle V_0 \rangle$ were averaged over the entire sampling period for each operating condition. The free-stream measurements were averaged in this way to minimize uncertainty introduced by the convection of turbulence from the sampling location to the rotor plane. These averaging methods produced a set of cycle-average performance coefficients and tip-speed ratios for every nominal operating condition. The median of each set of cycle-average values was taken as the representative C_P, C_T, and λ, and the interquartile range was taken as the uncertainty.

At each facility, the turbines were tested over the range of tip-speed ratios that produced net power. The desired tip-speed ratios were achieved by controlling the angular velocity of the turbines while maintaining an approximately constant free-stream velocity. Under this type of control, the measured torque was equal to the hydrodynamic torque produced by the rotor [40]. The cross-flow turbine's forces, torque, and angular position were sampled at a frequency of 1 kHz. The axial-flow performance was sampled at approximately 50 Hz. Free-stream velocity data were collected at 64 Hz for all tests.

2.5. Wake characterization

One of the blockage corrections considered in this study requires information about the wake structure. Because these data were time-intensive to collect, wake measurements were taken only at the tip-speed ratio corresponding to the peak power coefficient. Wake data were collected at 100 Hz using two acoustic Doppler velocimeters mounted on a three-axis, motorized gantry. For both turbines, measurements were taken at 0.75, 1.25, 1.75, and 2.25 diameters downstream of the center of the rotor. At each downstream location, the measurement grid consisted of a single horizontal traverse in the cross-stream direction, with measurements spaced 0.01 m apart. The traverses were centered vertically relative to the turbine rotor. Fig. 2 illustrates the wake measurement locations for the cross-flow turbine. A similar grid was used for the axial-flow turbine. Raw measurements were despiked using the method of Goring and Nikora [41], and data points with low correlation values were discarded [42]. These measurements were used to estimate the cross-sectional area of the wake (A_1) downstream of each turbine. The values of A_1 were determined by calculating the position, in the cross-stream direction, of the boundary between the core flow (fluid that passed through the turbine) and bypass flow (fluid that passed around the turbine). This boundary was taken as the point where the velocity in the core flow equaled

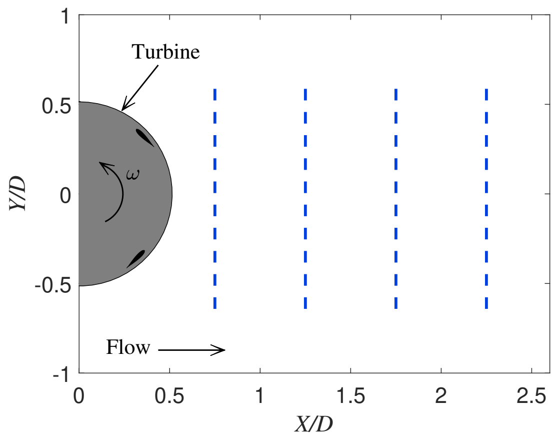

Fig. 2. Top view of the measurement grid used to collect wake data for the cross-flow turbine. The dashed lines show the location of each cross-stream traverse.

or exceeded the free-stream velocity. According to theory, A_1 is measured at the streamwise location where the pressure between the core and bypass flows reaches equilibrium. This point is ambiguous without spatially-resolved pressure measurements, which were not available for these tests. Therefore, the wake area was estimated at each of the streamwise locations shown in Fig. 2. All four values were used in the analytical correction, and the one which yielded the lowest error was reported.

3. Analytical methods

Blockage corrections applied to confined performance data estimate the equivalent unconfined power coefficient (C'_P), thrust coefficient (C'_T), and tip-speed ratio (λ'),

$$C'_P = \frac{P'}{\frac{1}{2}\rho A_T V_0'^3}, \tag{4}$$

$$C'_T = \frac{T'}{\frac{1}{2}\rho A_T V_0'^2}, \tag{5}$$

$$\lambda' = \frac{R\omega'}{V'_0}, \tag{6}$$

where the prime denotes an unconfined value. The methods considered in this section are based on axial momentum theory applied to an actuator disc in either closed channel flow (representative of a closed-section wind tunnel or cavitation tunnel with no free surface) or open channel flow (representative of a flume with a deformable free surface). These methods are not suitable for open-jet wind tunnels.

3.1. Glauert's method

Although we do not directly evaluate the original propeller blockage correction developed by Glauert [2], all of the methods considered in this section are based, to a varying degree, on his analysis. The assumptions that underpin Glauert's derivation are that the incoming flow is uniform, the propeller (or turbine) is two-dimensional and has an infinite number of frictionless blades, thrust over the entire rotor is uniform, the wake does not rotate, and the effects of boundary proximity and channel aspect ratio are insignificant.

Given performance data collected at a constant operating condition in confined flow, Glauert's method computes V_0', the free-stream velocity that, in an unconfined flow, would produce the same values of thrust and stream-wise velocity through the rotor (u_T) at the same angular velocity, i.e.,

$$T' = T, \tag{7}$$

$$u_T' = u_T, \tag{8}$$

$$\omega' = \omega. \tag{9}$$

Glauert does not specifically address power, but to correct C_P, subsequent authors have invoked the definition of power absorbed by an actuator disc,

$$P = T u_T. \tag{10}$$

Combining Eqs. (7), (8), and (10) yields

$$P' = P. \tag{11}$$

Dividing Eqs. (4)-(6) by Eqs. (1)-(3), respectively, and using the equalities in Eqs. (7), (9), and (11) yields expressions for C_P', C_T', and λ' as functions of V_0':

$$C_P' = C_P\left(\frac{V_0}{V_0'}\right)^3, \tag{12}$$

$$C_T' = C_T\left(\frac{V_0}{V_0'}\right)^2, \tag{13}$$

$$\lambda' = \lambda\left(\frac{V_0}{V_0'}\right). \tag{14}$$

For a turbine, blockage increases u_T for a given V_0. Therefore, the free-stream velocity that gives the same u_T in an unconfined flow is typically higher (i.e., $V_0' > V_0$). By calculating the equivalent unconfined power coefficient, thrust coefficient, and tip-speed ratio using V_0', Glauert's correction can account for the performance increase that a turbine experiences in confined flow.

The equivalent unconfined free-stream velocity V_0' is estimated by first applying the principles of continuity, conservation of axial momentum, and the Bernoulli equation to an actuator disc in confined flow. This yields a system of four equations,

$$u_T A_T = u_1 A_1, \tag{15}$$

$$u_2(A_C - A_1) = V_0 A_C - u_T A_T, \tag{16}$$

$$T = \frac{1}{2}\rho A_T(u_2^2 - u_1^2), \tag{17}$$

$$T + \frac{1}{2}\rho A_C(V_0^2 - u_2^2) = \rho A_1 u_1(V_0 - u_1) + \rho(A_C - A_1)u_2(V_0 - u_2), \tag{18}$$

where u_1 is the velocity of the core flow and u_2 is the velocity of the bypass flow. It should be noted that Eqs. (15)-(18) apply to an actuator disc that extracts energy from the flow (i.e., a turbine). Therefore, the thrust in Eqs. (17) and (18) is oppositely signed from the thrust in Glauert's original derivation, which applies to an actuator disc that adds energy to the flow (i.e., a propeller). Assuming u_T has been estimated from Eqs. (15)-(18), the unconfined free-stream velocity can then be found by introducing a fifth equation: the expression for thrust in unconfined flow obtained from momentum conservation,

$$T' = 2\rho u_T' A_T(V_0' - u_T'). \tag{19}$$

Combining Eqs. (2), (7), and (8) with Eq. (19) yields a solution for V_0':

$$V_0' = \frac{V_0((u_T/V_0)^2 + C_T/4)}{u_T/V_0}. \tag{20}$$

Once V_0' is known, the unconfined coefficients C_P', C_T', and λ' can be calculated for each operating point using Eqs. (12)-(14).

Specific corrections for a turbine operating in closed or open channel flow, as presented by Barnsley and Wellicome [19], Mikkelsen and Sørensen [20], Werle [21], and Houlsby et al. [22] are described separately in the following sections. The correction given by Maskell [29] for bluff bodies is contrasted in Section 5.5.

3.2. Closed channel flow

Several methods have been proposed to account for the effects of blockage in a channel without a free surface. All methods reference the streamtube model shown in Fig. 3. The first method, developed by Barnsley and Wellicome [19] and introduced to the marine energy research community by Bahaj et al. [12], applies Glauert's axial momentum theory analysis [2] to a turbine rather than a propeller. A second method, developed by Mikkelsen and Sørensen [20], also follows Glauert's analysis. However, it provides an alternative closure to the correction presented by Barnsley and Wellicome. A third method, derived by Werle [21], applies simplifying approximations to Glauert's theory.

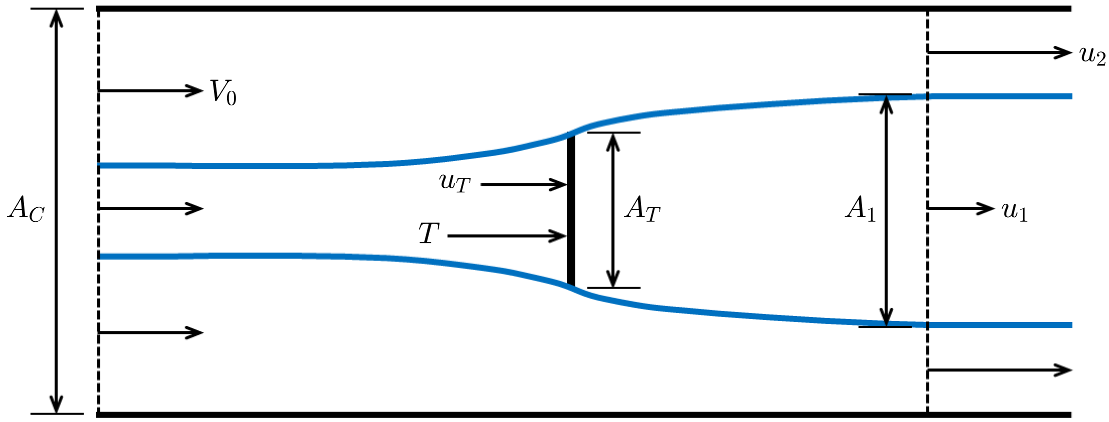

Fig. 3. Streamtube model of an actuator disc in closed channel flow with no free surface.

3.2.1. Barnsley and Wellicome's method

To apply the correction given by Barnsley and Wellicome [19] (BW), measurements of A_T, A_C, V_0, T, and ρ must be available. If so, Eqs. (15)-(18) become a closed system with four unknowns: A_1, u_T, u_1, and u_2. Although a compact analytical solution to these equations does not exist, individual solutions can be obtained for certain operating conditions. By rearranging Eqs. (15)-(18), an iterative scheme is developed to solve for the ratio u_T/V_0. This scheme consists of three equations:

$$\frac{u_T}{u_1} = \frac{-1 + \sqrt{1 + \beta((u_2/u_1)^2 - 1)}}{\beta(u_2/u_1 - 1)}, \tag{21}$$

$$\frac{V_0}{u_1} = \frac{u_2}{u_1} - \beta\left(\frac{u_T}{u_1}\right)\left(\frac{u_2}{u_1} - 1\right), \tag{22}$$

$$\frac{V_0}{u_1} = \sqrt{\frac{(u_2/u_1)^2 - 1}{C_T}}. \tag{23}$$

The solution is found by guessing a reasonable value for u_2/u_1 and solving Eq. (21) for u_T/u_1. Using these values of u_2/u_1 and u_T/u_1, Eqs. (22) and (23) can be solved for the ratio V_0/u_1. If the two values of V_0/u_1 do not match, a new value of u_2/u_1 should be selected, and the scheme repeated until the error between Eqs. (22) and (23) is minimized. Note that solutions only exist for values of the input parameters that yield physical results, e.g., $u_2 > u_T > u_1$, $V_0 > u_T$, and $u_2 > V_0$. With u_T/u_1 and V_0/u_1 known, the ratio u_T/V_0 can be found. Given u_T/V_0, V_0' can be calculated using Eq. (20), and C_P', C_T', and λ' can be estimated at each operating point using Eqs. (12)-(14). A summary of this method is presented by Bahaj et al. [12] and derived by Kinsey and Dumas [11]. While the original technical report [19] does not appear to be publicly available, given limited comments on blockage corrections in subsequent work [43], the primary reference is unlikely to contain more detail than is presented in the secondary sources.

3.2.2. *Mikkelsen and Sørensen's method*

Mikkelsen and Sørensen [20] (MS) proposed a correction that presents an alternative closure to Eqs. (15)-(18). As with Barnsley and Wellicome's correction, it is assumed that A_T, A_C, V_0, and ρ are known. However, A_1 is measured rather than T. This method rearranges Eqs. (15)-(18) to solve for the unknown parameters u_T, u_1, u_2, and C_T directly, with no iteration required. Even if measurements of T or C_T are available, they should not be used in conjunction with this method, as the system of equations would become overdetermined. The correction consists of the following four equations:

$$u_T = \frac{V_0(A_1/A_T)(\beta(A_1/A_T)^2 - 1)}{\beta(A_1/A_T)(3A_1/A_T - 2) - 2A_1/A_T + 1}, \quad (24)$$

$$u_1 = \frac{u_T A_T}{A_1}, \quad (25)$$

$$u_2 = \frac{A_T(V_0 - \beta u_T)}{A_T - \beta A_1}, \quad (26)$$

$$C_T = \frac{u_2^2 - u_1^2}{V_0^2}. \quad (27)$$

Once u_T and C_T have been calculated, the unconfined velocity V_0' can be found using Eq. (20) and the unconfined turbine performance parameters calculated using Eqs. (12)-(14). This method highlights the fact that Eqs. (15)-(18) can be solved multiple ways, as long as adequate measurements are available to close the system.

3.2.3. *Werle's method*

The final closed channel blockage correction considered in this study was developed by Werle [21]. This method is also based on Eqs. (15)-(18) but makes several approximations that allow the unconfined parameters C_P', C_T', and λ' to be calculated as functions of the blockage ratio alone, without an intermediate calculation of V_0'. These approximations are given as

$$\frac{C'_P}{C'_{P,max}} \approx \frac{C_P}{C_{P,max}}, \tag{28}$$

$$\frac{C'_T}{C'_{T,max}} \approx \frac{C_T}{C_{T,max}}, \tag{29}$$

$$\frac{u'_T}{u'_{T,max}} \approx \frac{u_T}{u_{T,max}}, \tag{30}$$

where the expressions for $C'_{P,max}$, $C'_{T,max}$, and $u'_{T,max}$ are given by the well-known Betz criterion [44, 45], and the expressions for $C_{P,max}$, $C_{T,max}$, and $u_{T,max}$ are given by Garrett and Cummins [3]. Substituting these expressions into Eqs. (28)-(30) gives corrections for C_P, C_T, and u_T, which Werle presents as

$$C'_P \approx C_P(1-\beta)^2, \tag{31}$$

$$C'_T \approx C_T\frac{(1-\beta)^2}{(1+\beta)}, \tag{32}$$

$$\frac{u'_T}{V'_0} \approx \frac{u_T}{V_0}(1-\beta). \tag{33}$$

Applying Eqs. (8) and (14) to Eq. (33) yields an expression in terms of the tip-speed ratio,

$$\lambda' \approx \lambda(1-\beta). \tag{34}$$

Based on an independent re-derivation of Werle's method, Eqs. (33) and (34) appear to contain sign errors and are inconsistent with the rest of the model. If treated consistently, the equations should be given as

$$\frac{u'_T}{V'_0} \approx \frac{u_T}{V_0}(1+\beta), \tag{35}$$

$$\lambda' \approx \lambda(1+\beta). \tag{36}$$

However, because the purpose of this study is to evaluate blockage corrections as presented in the literature, the tip-speed ratio correction given by Eq. (34) was applied to our experimental data without modification.

3.3. Open channel flow (Houlsby et al.'s method)

An analytical model for an actuator disc in flow with a deformable free surface was first developed by Houlsby et al. [22] (Houlsby). As with Glauert's model for closed channel

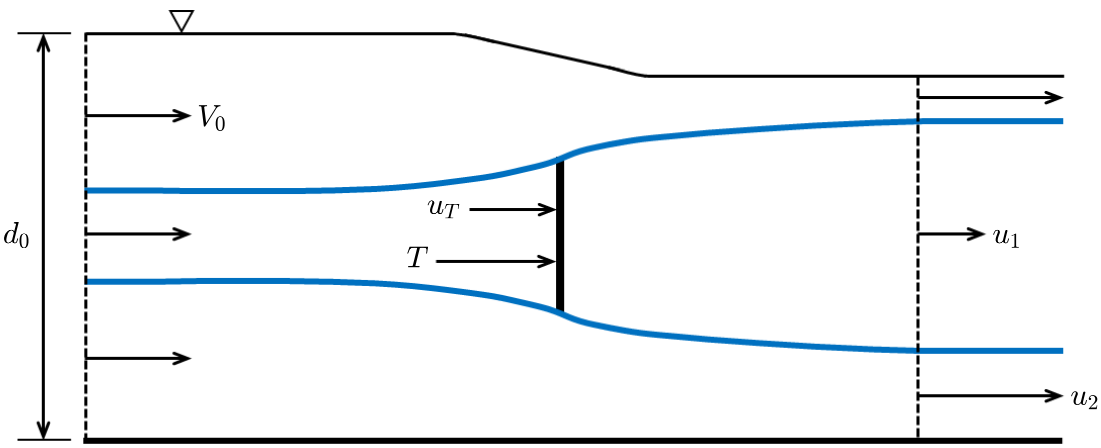

Fig. 4. Streamtube model of an actuator disc in open channel flow with a deformable free surface.

flow, this model was derived by applying continuity, conservation of axial momentum, and the Bernoulli equation to an actuator disc in confined flow. However, the free surface of the flow was allowed to deform, as shown in Fig. 4. This yields seven equations, which can be rearranged and expressed as a system of two equations:

$$u_1 = \frac{Fr^2u_2^4 - (4 + 2Fr^2)V_0^2u_2^2 + 8V_0^3u_2 - 4V_0^4 + 4\beta C_T V_0^4 + Fr^2V_0^4}{-4Fr^2u_2^3 + (4Fr^2 + 8)V_0^2u_2 - 8V_0^3}, \tag{37}$$

$$u_1 = \sqrt{u_2^2 - C_T V_0^2}. \tag{38}$$

As with the closed channel model, analytical solutions to Eqs. (37) and (38) do not exist. However, specific solutions can be found using an iterative method. To apply the correction, measurements of A_T, A_C, V_0, T, ρ, and d_0 are required. The solution method consists of guessing a reasonable value for u_2, solving Eqs. (37) and (38) separately for u_1, and iterating until the two values of u_1 are equal. With u_1 and u_2 known, the stream-wise velocity through the turbine can be calculated as

$$u_T = \frac{u_1(u_2 - V_0)(2gd_0 - u_2^2 - u_2V_0)}{2\beta gd_0(u_2 - u_1)}. \tag{39}$$

The unconfined free-stream velocity and turbine performance parameters can then be found from Eqs. (20) and (12)-(14).

This open channel flow model is referenced by Whelan et al. [26] and Houlsby and Vogel [4]. Whelan et al. [26] used this model as the basis for a blockage correction that can be applied within a blade element momentum code. Houlsby and Vogel [4] explored solutions to this model over a range of operating conditions. However, to our knowledge, it has not previously been cast as an analytical blockage correction.

3.4. Summary of analytical methods

All of the blockage corrections considered in this section are grounded in Glauert's derivation [2]. In his original work, Glauert presented a set of equations that can be used to solve for V_0' and, therefore, calculate the equivalent unconfined turbine performance coefficients. Glauert also proposed a linearization of this model that provides a simpler method of estimating V_0' when the blockage ratio is less than 0.15. While Glauert's derivation applies to propellers, it can easily be adapted to turbines by reversing the direction of thrust to yield Eqs. (15)-(20).

The corrections given by Barnsley and Wellicome [19] and Mikkelsen and Sørensen [20] use measured quantities to solve Eqs. (15)-(18) for unknown parameters, calculate V_0' using Eq. (20), and estimate the unconfined performance coefficients using Eqs. (12)-(14). The only difference between these two methods is Barnsley and Wellicome's use of thrust to close the system and Mikkelsen and Sørensen's use of the wake area. The correction presented by Werle [21] uses expressions for the maximum theoretical power coefficient and corresponding thrust coefficient and stream-wise velocity through the rotor in confined and unconfined flow. Although Werle's correction is based on Glauert's theory, it relies on assumptions that yield a model distinct from the other closed channel corrections. The open channel flow model given by Houlsby et al. [22] is a generalization of Eqs. (15)-(18) to allow for a deformable free surface. So, if the free surface does not deform, Houlsby et al.'s correction reduces to the model used by Barnsley and Wellicome and Mikkelsen and Sørensen.

3.5. Estimation of correction error

The effectiveness of each blockage correction was evaluated by a measure of the difference between the corrected $C_P(\lambda)$ and $C_T(\lambda)$ curves relative to the unconfined performance curves. This error metric was computed as the projection of the Euclidean distance (positive definite scalar quantity) between uniformly sampled points on the corrected and unconfined curves into C_P, C_T, or λ space. These distances were then normalized by the corresponding values on the unconfined curves to calculate a relative error. The mean of these values, over all operating conditions that produced net power, was taken as an estimate of correction error. Since Mikkelsen and Sørensen's method required wake data, it was applied only at the tip-speed ratio corresponding to the peak power coefficient. Therefore, the error of each method was estimated at this single point as well.

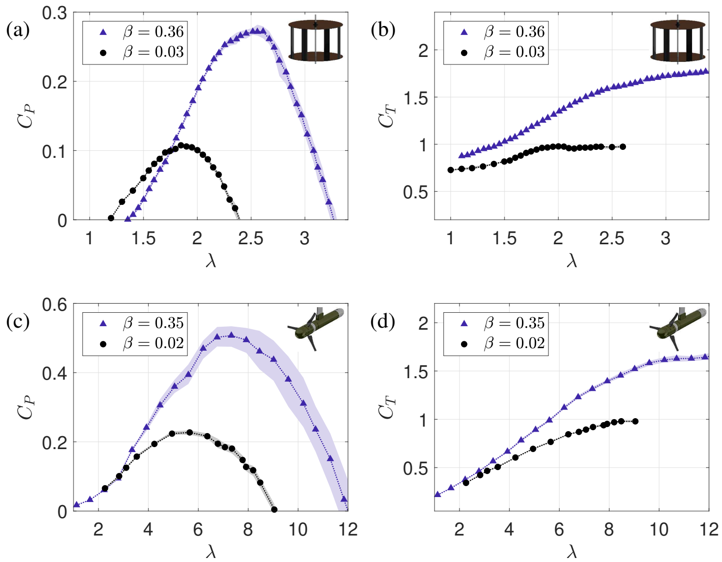

Fig. 5. Confined and unconfined power and thrust coefficients for the cross-flow (a, b) and axial-flow (c, d) turbines. The shading represents the measurement uncertainty at each tip-speed ratio, as estimated from the interquartile range of cycle-average performance. In some instances, the uncertainty range is smaller than the plot markers, and therefore not visible.

4. Results

4.1. Performance and wake characteristics

The power and thrust coefficients measured under confined and unconfined conditions [46] are shown in Fig. 5. For both turbines, blockage produces a higher peak power coefficient at an elevated tip-speed ratio. Furthermore, the thrust coefficient at the point of peak C_P is increased, and the turbines produce net power over a wider range of tip-speed ratios. These results are in agreement with previous findings [6]. Interestingly, the overall trend of an increased C_P at high blockage reverses or becomes negligible at lower tip-speed ratios. Past studies have reported an insensitivity of C_P to blockage at low tip-speed ratios for both cross-flow and axial-flow turbines [6, 8, 11]. For cross-flow turbines, Consul et al. [6] and Kinsey and Dumas [11] attribute this to the effects of dynamic stall. Cross-flow turbines experience a range of angles of attack throughout a single revolution. At lower tip-speed ratios, the angles of attack undergo higher fluctuations, which can lead to dynamic stall. As blockage increases, the flow speed through the rotor tends to increase as well, decreasing the effective tip-speed ratio and further encouraging dynamic stall. Therefore, any gains in C_P caused by higher flow speeds through the rotor are negated by increased dynamic stall. However, as shown in Fig. 5, an increased blockage ratio has a negative, rather than neutral, effect on the power coefficient of the cross-flow turbine at

Table 1
Non-dimensional wake area (A_1/D) at four stream-wise locations (X/D).

X/D	0.75	1.25	1.75	2.25
Cross-flow turbine	1.10	1.14	1.16	1.19
Axial-flow turbine	1.11	1.11	1.11	1.06

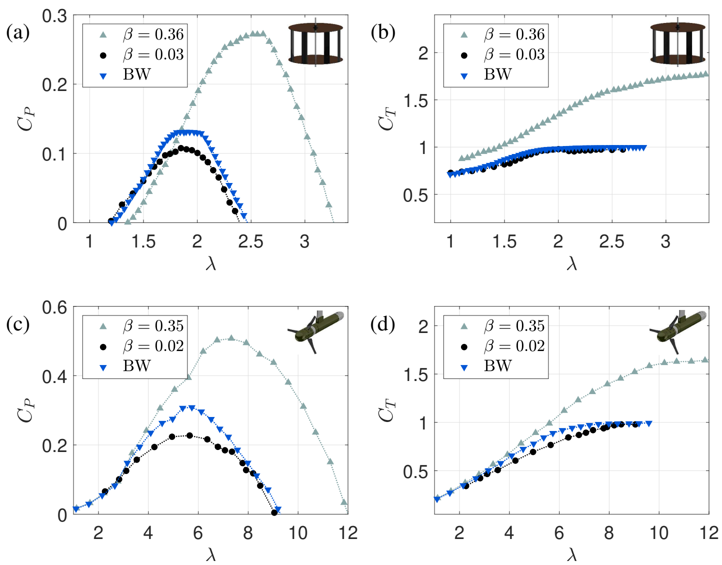

Fig. 6. Application of Barnsley and Wellicome's correction to the confined performance data from the cross-flow (a, b) and axial-flow (c, d) turbines.

low tip-speed ratios. As prior studies are based on numerical simulations, this discrepancy could be explained by the difficulty of accurately modeling dynamic stall.

As described in Section 2.5, the cross-sectional area of the wake downstream of both turbines was estimated from velocity measurements. Table 1 presents the values of A_1, nondimensionalized by turbine diameter, at each of the four stream-wise positions shown in Fig. 2. These values were used only when applying Mikkelsen and Sørensen's correction.

4.2. Application of blockage corrections

4.2.1. Barnsley and Wellicome's method

Fig. 6 presents the results of applying Barnsley and Wellicome's correction to the confined data. The uncorrected, confined data are superimposed for reference. If the correction had worked perfectly, the corrected data would have collapsed onto the uncon-

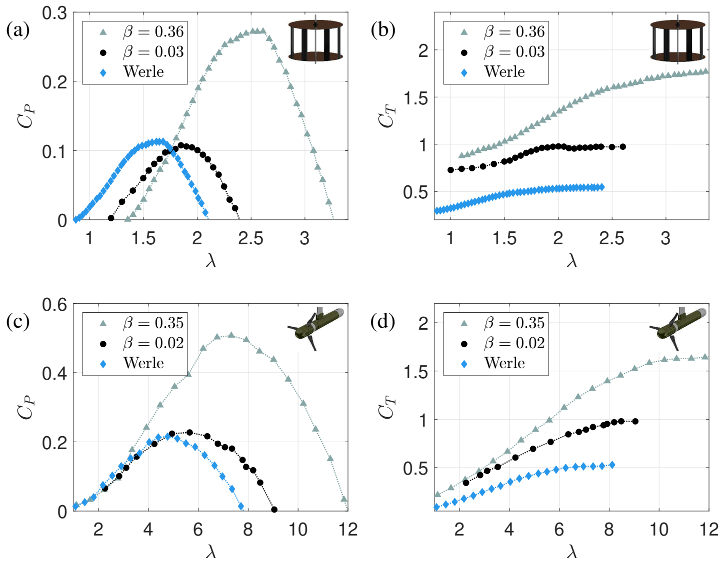

Fig. 7. The results of applying Werle's correction to the confined performance data from the cross-flow (a, b) and axial-flow (c, d) turbines.

fined performance curve. Although some discrepancies remain, the correction generally accounts for the effects of blockage on the power and thrust coefficients of both turbines.

4.2.2. Werle's method

Fig. 7 shows the application of Werle's correction to the confined performance data. Although the correction performs adequately for the magnitude of the power coefficient, it significantly over-corrects the thrust coefficient and tip-speed ratio. As mentioned in Section 3.2.3, the tip-speed ratio correction given by Eq. (34) is not consistent with the rest of the derivation. However, the modified form given by Eq. (36) further reduces the corrected tip-speed ratios, increasing the disagreement between corrected and unconfined performance (not shown).

4.2.3. Houlsby et al.'s method

Fig. 8 presents the results of Houlsby et al.'s correction which, unlike the previous two methods, allows for a deformable free surface. The results of this correction are almost identical to those from Barnsley and Wellicome's method (Fig. 6).

4.2.4. Mikkelsen and Sørensen's method

Fig. 9 gives the results of applying Mikkelsen and Sørensen's correction. Unlike the previous methods, a single operating point (peak C_P) was evaluated rather than the

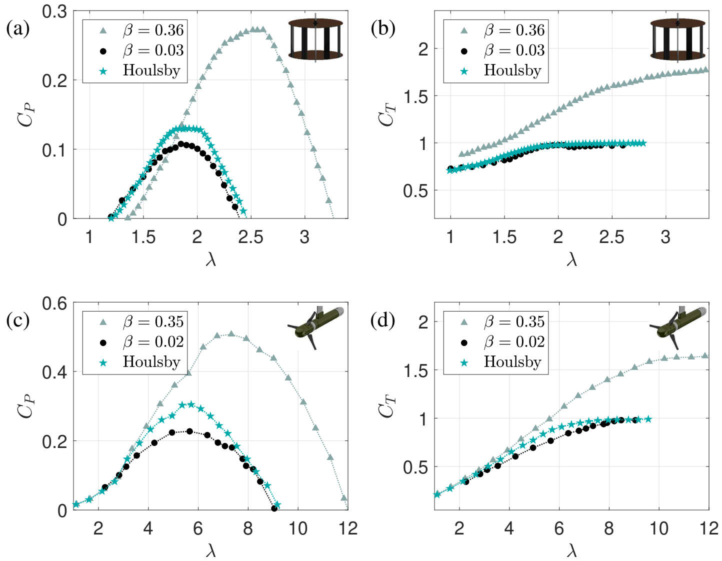

Fig. 8. Houlsby et al.'s method applied to the confined performance data from the cross-flow (a, b) and axial-flow (c, d) turbines.

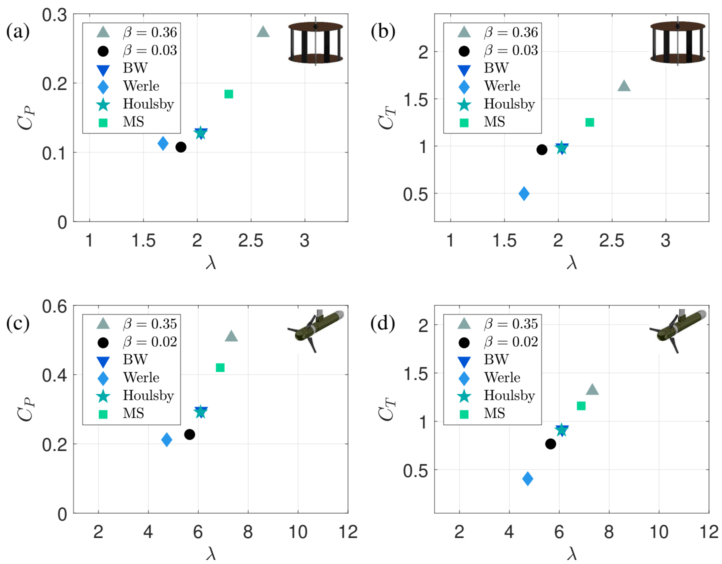

Fig. 9. Overall correction performance at tip-speed ratios corresponding to peak C_P for cross-flow (a, b) and axial-flow (c, d) turbines. Mikkelsen and Sørensen's correction is for the downstream wake measurement that gave the closest correction to unconfined data. The closer the corrected performance is to unconfined measurements (black circle), the more effective the correction. Uncorrected performance is shown for reference (gray triangle).

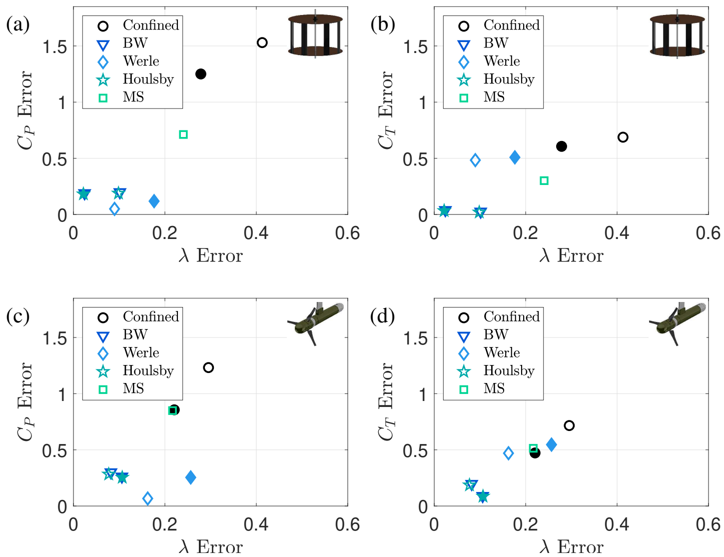

Fig. 10. Blockage correction error for the cross-flow (a, b) and axial-flow (c, d) turbines, relative to unconfined data. Filled markers indicate error averaged over full curves, while open markers indicate error at peak C_P.

full C_P and C_T curves, as wake data could not be collected in a timely manner for all operating conditions. All of the values for A_1 presented in Table 1 were evaluated, and it was determined that $X/D = 2.25$ gave the least error for the cross-flow turbine and $X/D = 1.75$ gave the least error for the axial-flow turbine. For comparison, the results of applying the other corrections to the peak C_P of each turbine are also shown in Fig. 9.

5. Evaluation of blockage corrections

The errors for all blockage corrections applied to both turbines are summarized in Fig. 10. For reference, the equivalent calculation for the confined, uncorrected data (i.e., performance change as a consequence of blockage) is given as well. The ratio of A_S to A_T was less than 5% under confined conditions for both turbines, so alternative definitions of the blockage ratio, such as $\beta = A_T/(A_C - A_S)$, do not significantly affect the values shown in Fig. 10.

5.1. Full performance curve

As quantified in Fig. 10, Houlsby et al.'s and Barnsley and Wellicome's methods are relatively effective at correcting for blockage over the entire range of tip-speed ratios considered for both turbines. These corrections give almost identical results, with Houlsby et al.'s method performing slightly better overall. This outcome is to be expected, given that Houlsby et al.'s analytical model is a generalization of the one used by Barnsley and Wellicome to allow for a deformable free surface. Since no significant free surface deformation was observed during these experiments, it is unsurprising that the two methods yield similar outcomes.

Werle's method produces mixed results. The C_P correction performs better than or equal to Houlsby et al.'s and Barnsley and Wellicome's for both turbines and the C_T and λ corrections perform significantly worse. These outcomes are consistent with the original derivation [21]. As mentioned in Section 3.2.3, Werle's correction begins with the analytical expressions for $C_{P,max}$, $C_{T,max}$, and $u_{T,max}$ in both confined and unconfined flow [3, 44, 45]. These expressions yield corrections that are applicable only at the peak C_P. To generalize the corrections to other operating conditions, the approximations given in Eqs. (28)-(30) are used. However, the approximation for C_P given by Eq. (28) is the only expression that Werle mathematically justifies in the original derivation. This is done using a "correlation scheme" that is attributed to Werle and Presz [47]. Repeating this method for C_T and u_T reveals that the approximations given in Eqs. (29) and (30) are less well justified than Eq. (28). This could explain why Werle's C_P correction performs better than the C_T or λ corrections.

5.2. Peak C_P

Considering only the results for the peak C_P allows a comparison of all four blockage corrections. The errors in Houlsby et al.'s, Barnsley and Wellicome's, and Werle's methods follow the same trends as the full curve error. Mikkelsen and Sørensen's method yields much higher errors than either Houlsby et al.'s or Barnsley and Wellicome's correction. This result is unexpected given that Barnsley and Wellicome's and Mikkelsen and Sørensen's corrections use the same set of equations and differ only in their choice of input parameters (thrust versus wake area). The poor performance of Mikkelsen and Sørensen's method is likely due to the difficulty of measuring A_1 in experiment. The horizontal traverses shown in Fig. 2 captured the size of the wakes in only one dimension, while wakes have a higher dimensional structure (e.g., Bachant and Wosnik [37], for cross-flow turbines). Additionally, due to experimental limitations, the wake data were collected at water temperatures of 11°C for the cross-flow turbine and 17°C for the axial-flow turbine, compared to 22°C and 20°C for the performance data. It is uncertain how these changes in temperature, which impact the Reynolds number, would affect the wake, though prior results have suggested that wake structure reaches Reynolds independence sooner than turbine performance [31]. Compounding the difficulty of accurately measuring A_1, the correction is quite sensitive to this parameter. An error of ±10% in the value of A_1 produces an error of approximately ±32% in Mikkelsen and Sørensen's C_P correction. By comparison, introducing a ±10% error into the value of T produces an error of ±12% when applying Barnsley and Wellicome's C_P correction to the same data. Although Mikkelsen and Sørensen's correction did not perform well in this study, its performance should improve if a better estimate of A_1 were available. However, in experiments, it is unlikely that such a measurement would be simpler than measuring the rotor thrust. The fact that Barnsley and Wellicome's and Mikkelsen and Sørensen's corrections give different results, despite solving the same equations, illustrates that the choice of input parameters can significantly influence the magnitude of the correction.

5.3. Impact of Reynolds number

Due to experimental limitations, both turbines were operated in a transitional regime, where performance was dependent on Reynolds number [31–33]. Because blockage increases the stream-wise flow speed through the rotor plane, the turbines experienced an elevated "local" Reynolds number (Re_L, calculated using u_T as the characteristic velocity) under confined conditions, even as the free-stream Reynolds number was held constant. Specifically, momentum theory suggests that, due to blockage, the Re_L of the cross-flow turbine increased by about 9% and the Re_L of the axial-flow turbine by about 7%. Although these increases are relatively small, they can meaningfully change turbine performance [48]. Because blockage corrections are implicitly Reynolds independent, changes in Re_L are likely to increase the correction error when experiments are conducted below Reynolds independence. This provides two further insights into the accuracy of Houlsby et al.'s and Barnsley and Wellicome's methods reported here.

First, both Houlsby et al.'s and Barnsley and Wellicome's corrections are more effective for the cross-flow turbine than the axial-flow turbine. This is unexpected, considering blockage corrections were originally derived for axial-flow devices. Furthermore, prior work has indicated that Barnsley and Wellicome's correction performs better for axial-flow turbines [11]. This discrepancy may be explained by Reynolds dependence. Although the axial-flow turbine saw a slightly smaller increase in local Reynolds number under confined conditions, it was operating at a lower free-stream Reynolds number (Re_c = 14 000) than the cross-flow turbine (Re_c = 31 000) and was likely further from Reynolds independence. Therefore, the change in Re_L is expected to have a larger effect on the axial-flow turbine. To evaluate this hypothesis, it would be necessary to characterize trends in the performance of both turbines as a function of Reynolds number, which was beyond the scope of this study.

Second, Houlsby et al.'s and Barnsley and Wellicome's corrections are more accurate for the thrust coefficient than the power coefficient. This may also be due, at least in part, to Reynolds number dependency. In unrelated experiments, both turbines were tested in the UW flume at two different transitional Reynolds numbers. These results are shown in

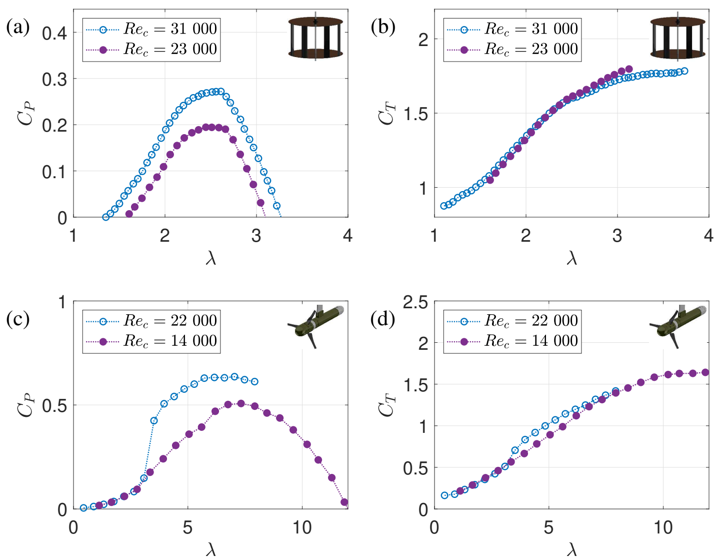

Fig. 11. Power and thrust coefficient curves for the cross-flow (a, b) and axial-flow (c, d) turbines at multiple transitional Reynolds numbers in the UW flume. The power coefficients are more sensitive to variations in Reynolds number than the thrust coefficients.

Fig. 11. The cross-flow turbine's power coefficient changed significantly with Reynolds number around the conditions referenced in this study. However, the thrust coefficient was relatively insensitive to Reynolds number, such that corrections for C_T would not be significantly impacted by the changes in Re_L. The axial-flow turbine performance followed a similar trend.

5.4. Impact of model limitations

Axial momentum theory applied to an actuator disc is a significant simplification of real turbine dynamics. As noted by Houlsby and Vogel [4], axial momentum theory is not restricted to turbines of a certain shape. However, the assumptions that underpin the theory, discussed in Section 3.1, do not hold for most real turbines, either axial-flow or cross-flow. Several past studies have noted that these limitations reduce blockage correction efficacy [11, 16, 23, 25]. Here, we discuss several of these limitations in the context of our experimental results.

With the exception of Werle's method, the thrust coefficient corrections are more effective than the power coefficient corrections. Axial momentum theory does not account for any rotation, either of the turbine or of the wake. While expressions for thrust can be derived without this information, power is equal to torque multiplied by the angular velocity of the turbine. Therefore, power from a real turbine requires rotation and an exchange of angular momentum between the rotor and the flow. Most blockage corrections based on axial momentum theory assume power is the product of thrust and the stream-wise flow speed through the rotor. This expression is inaccurate for several reasons. First, the power absorbed by an actuator disc does not account for the presence of rotational kinetic energy in the wake. Second, although axial momentum theory assumes a frictionless turbine, drag on rotating components reduces the torque produced by the rotor. This is accounted for in measured torque but is not reflected in axial momentum theory. Finally, thrust measurements may include components of the system that do not produce torque, such as the hub or support structure. These factors mean that real power is not generally the product of T and u_T. Therefore, because thrust can be expressed directly by axial momentum theory, whereas power can only be estimated, it is expected that corrections based on axial momentum theory would perform better for C_T than for C_P. This hypothesis is supported by the results of our experimental assessment (Fig. 10). To overcome this limitation, a blockage correction originating from angular momentum theory would be required.

Examining the limitations of axial momentum theory may also explain why, as shown in Figs. 6 and 8, the C_P correction is more effective at lower and higher tip-speed ratios than in the center of the curve. As discussed previously, axial momentum theory neglects wake rotation. Therefore, it is expected that the corrections will perform better at operating conditions with minimal wake rotation. Because wake rotation is a reaction to the torque of the rotor, operating conditions that produce less torque also cause less wake rotation. These operating conditions correspond to lower and higher tip-speed ratios where torque and, consequently, C_P are reduced.

The fact that the corrections are based on axial momentum theory also has interesting implications for the tip-speed ratio. Glauert [2] specifies that the angular velocity of the turbine and the flow speed through the rotor remain constant between the confined and equivalent unconfined conditions. With wake rotation neglected, this justifies the assertion that the thrust remains constant as well. However, because the correction is based on axial momentum theory, the calculation of V_0' does not depend on ω. Aside from providing a justification for constant thrust between confined and unconfined conditions, the requirement that $\omega' = \omega$ is used only to derive Eq. (14), the tip-speed ratio correction. Because axial momentum theory does not directly address rotation, prior work [25] has questioned whether the equivalent unconfined condition should be that which gives the same angular velocity or the same tip-speed ratio. We chose to assume $\omega' = \omega$ and correct the tip-speed ratio according to Eq. (14), which is in line with Glauert's statements and gives good agreement with the unconfined results.

5.5. Maskell's bluff body correction

Another relevant restriction of axial momentum theory is that it becomes invalid when the unconfined thrust coefficient exceeds unity, as this corresponds to reversed flow in the wake. As shown in Fig. 5, the unconfined thrust coefficients of the cross-flow and axial-flow turbines tested in this study were within this threshold. However, this is not always the case, motivating the use of a blockage correction based on bluff body theory for highly loaded turbines. As discussed in Section 1, two prior studies applied a blockage correction based on the theory of Maskell [29] to an axial-flow turbine [26] and a cross-flow turbine [11]. Both studies found that Maskell's correction performed better than actuator disc methods for highly loaded turbines.

Maskell observed that blockage corrections based on actuator disc theory were inadequate for objects that produced a bluff body wake. Maskell's blockage correction is based on momentum theory coupled with an empirical description of wake behavior. The derivation assumes that the bluff body wake is axisymmetric, the flow is uniform and unidirectional, and the blockage ratio is small, such that higher-order terms of β can be neglected. The correction calculates the free-stream velocity ($V'_{0,b}$) that, in an unconfined flow, would produce the same flow speed past the object ($u_{2,b}$). Note that $u_{2,b}$ is the velocity of the shear layer downstream of the bluff body and is distinct from u_2, the velocity of the bypass flow in actuator disc theory. Given measurements of $u_{2,b}$, $V_{0,b}$, C_T, and β, the ratio $u'_{2,b}/V'_{0,b}$ can be calculated according to

$$\frac{(u_{2,b}/V_{0,b})^2}{(u'_{2,b}/V'_{0,b})^2} = 1 + \frac{C_T\beta}{(u'_{2,b}/V'_{0,b})^2 - 1}. \tag{40}$$

With $u'_{2,b}/V'_{0,b}$ known, the equivalent unconfined thrust coefficient can be estimated as

$$C'_T = C_T\frac{(u'_{2,b}/V'_{0,b})^2}{(u_{2,b}/V_{0,b})^2}. \tag{41}$$

Since $u_{2,b} = u'_{2,b}$, Eq. (41) reduces to

$$C'_T = C_T\left(\frac{V_{0,b}}{V'_{0,b}}\right)^2. \tag{42}$$

Although this correction is similar in form to Eq. (13), the unconfined free-stream velocity is that which gives the same value of $u_{2,b}$ between confined and unconfined conditions, rather than u_T. To apply Maskell's correction as presented, it is necessary to have a measurement of $u_{2,b}$. As for Mikkelsen and Sørensen's correction, it would be difficult to identify an unambiguous location to sample this value for an experimental turbine.

Rather than applying Maskell's method exactly as formulated, past studies have applied a correction inspired by the theory. Whelan et al. [26] assumed that, when operating in a highly loaded condition, a turbine responds primarily to the bypass flow rather than the flow through the rotor plane. This allows C_T and λ to be corrected as

$$C'_T = C_T\left(\frac{V_0}{u_2}\right)^2, \tag{43}$$

$$\lambda' = \lambda\left(\frac{V_0}{u_2}\right). \tag{44}$$

Neither Whelan et al. [26] nor Kinsey and Dumas [11] attempt to estimate C'_P. Eqs. (43) and (44) are distinct from Maskell's original correction, in that they use the bypass velocity (u_2) as a correction factor, rather than the unconfined free-stream speed ($V'_{0,b}$). Furthermore, to apply Eqs. (43) and (44), Whelan et al. and, subsequently, Kinsey and Dumas estimate u_2 using actuator disc methods, despite assuming the operating conditions are such that actuator disc methods are invalid. Nevertheless, both past studies found that Eqs. (43) and (44) were more effective than actuator disc corrections when the rotors were more heavily loaded.

As the bypass flow adjacent to the rotor was not sampled in our experiments, we followed the method of Whelan et al. to correct C_T and λ using a Maskell-inspired approach. For the sake of investigation, we also corrected C_P as

$$C'_P = C_P\left(\frac{V_0}{u_2}\right)^3. \tag{45}$$

The results of applying Eqs. (43)-(45) to our confined performance data are shown in Fig. 12. The bypass velocity was estimated iteratively according to the method of Houlsby et al. Overall, Maskell's correction performs better at intermediate tip-speed ratios and worse at higher tip-speed ratios, which is in contrast to the results obtained by Whelan et al. and Kinsey and Dumas. Given that $u_2 > V'_0$, this approach makes a larger correction, which reduces some of the error we attribute to Reynolds dependence at the peaks of the C_P curves. The poor performance at higher tip-speed ratios is unexpected, as the thrust coefficients for both turbines in confined flow are similar to the values reported in Whelan et al. and Kinsey and Dumas. These mixed results suggest that a bluff body correction may be effective, but is not guaranteed to be more effective, even when the rotor is highly loaded. The physical justification for use is generally weaker than for axial momentum theory, and obtaining a correction factor directly in experiment is likely to be similarly problematic to obtaining the wake cross-sectional data necessary to apply Mikkelsen and Sørensen's correction. Consequently, a Maskell-inspired correction applied to experimental data may have a relatively large unquantified uncertainty. Finally, a Maskell-inspired

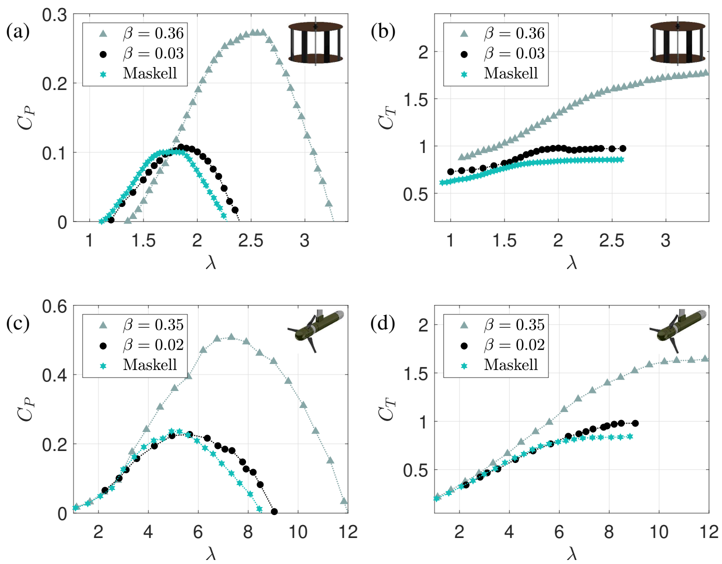

Fig. 12. Application of a blockage correction inspired by the bluff body theory of Maskell to the confined performance data from the cross-flow (a, b) and axial-flow (c, d) turbines.

correction does not resolve the fundamental mismatch between real turbine power and power absorbed by an actuator disk. This being said, prior studies [31, 49] have identified similarities between some turbine and bluff body wakes, suggesting that blockage corrections incorporating elements of bluff body theory could be more effective than those based purely on axial momentum.

5.6. Recommended blockage corrections

Analytical blockage corrections based on axial momentum theory are imperfect and can only provide estimates of the equivalent unconfined condition for performance data collected at high blockage. Although axial momentum theory solves for thrust directly, an approximate expression for power is required. Here, we demonstrate that for relatively high blockage, this leads to higher error in the C_P correction, which is unfortunate, as the power output of a turbine is often of greater interest than the loading. Despite the limitations of these methods, they do reduce the effects of blockage on performance data. Encouragingly, two of the methods resulted in less than 20% mean percentage error for the power coefficient of the cross-flow turbine tested at a blockage ratio of 0.36, experimental conditions that resulted in a change in the local Reynolds number and likely violated many of the assumptions of axial momentum theory. The same two methods gave less than 30% mean percentage error for the power coefficient of the axial-flow turbine tested at a blockage ratio of 0.35. It should be noted that the errors shown in Fig. 10 are specific to the turbines and test conditions in this study and should not be taken as indicative of the error associated with these blockage corrections for other turbine geometries or test conditions.

Of the corrections evaluated, we recommend the methods presented by Houlsby et al. and Barnsley and Wellicome. Houlsby et al.'s correction allows for a deformable free surface and gave slightly better results for this study, even though no significant free surface effects were observed. If thrust measurements are not available, but detailed wake data are, Mikkelsen and Sørensen's correction may be appropriate. However, given the correction's sensitivity to the wake area, we caution against general use in experiments. Even though Werle's correction performed best for the power coefficient, we do not recommend this method, due to inconsistencies in the underlying assumptions and poor performance for the tip-speed ratio and thrust coefficient. Corrections based on bluff body theory, such as the Maskell-inspired correction applied by Whelan et al. and Kinsey and Dumas, may be appropriate when methods based on axial momentum theory fail to converge, but they should be used with caution.

6. Conclusions

This study experimentally examined the effects of blockage on the performance of a cross-flow and an axial-flow turbine. Both turbines were characterized under conditions of high blockage and negligible blockage, while other significant parameters were held approximately constant. Overall, the effects of increased blockage on the turbines' power and thrust coefficients were consistent with prior investigations. These data were used to evaluate the performance of analytical blockage corrections for both turbine archetypes. Four of the five blockage corrections considered were based on axial momentum theory applied to an actuator disc in confined flow and followed the original propeller blockage correction presented by Glauert [2]. A correction based on momentum theory applied to a bluff body [29] was also evaluated. Interestingly, and in contrast to some prior results, we observed that the corrections were more effective for the cross-flow turbine than the axial-flow turbine. We hypothesize that this may be a consequence of changes in the local Reynolds number associated with our relatively high experimental blockage. This indicates that additional care should be taken when applying blockage corrections to data collected at transitional Reynolds numbers, which are common in a laboratory setting.

Our results also demonstrate that corrections for the thrust coefficient performed better than corrections for the power coefficient for both turbines. This is likely a combination of Reynolds number dependence and the limitations of axial momentum theory. Glauert's original blockage correction provides a system of equations, based on axial momentum theory, that can be used to calculate the equivalent unconfined free-stream velocity. However, his derivation does not explicitly mention how to apply this correction to measured performance coefficients. Subsequent studies have used his statement that the thrust, angular velocity of the turbine, and flow speed through the turbine remain constant between blocked and unblocked conditions to derive such corrections. However, this requires assuming that the power is given as the product of thrust and the flow speed through the turbine, which is inaccurate for real turbines. So, while thrust is calculated directly from axial momentum theory, power must be approximated, yielding higher error in the corrected power coefficients.

Despite the limitations of axial momentum theory, we have shown that analytical blockage corrections can give acceptable results for experimental data. However, the most effective way to eliminate blockage effects is to characterize turbine performance under approximately unconfined conditions, such that a blockage correction is unnecessary. Unfortunately, the model scales needed to reduce the effects of blockage are often at odds with the scales needed to achieve Reynolds independence. Large facilities allow testing at both low blockage ratios and high Reynolds numbers but present challenges for collecting well-controlled, high resolution measurements. Due to these limitations, certain experiments will necessarily be conducted in smaller facilities, and corrections will be required to account for the effects of blockage.

Based on our results, in addition to our evaluation of the corrections' ease of application and mathematical robustness, we recommend the methods presented by Barnsley and Wellicome [19] and Houlsby et al. [22]. We also note that the errors shown in Fig. 10 are specific to this study, and there is no guarantee that these corrections will give satisfactory results for an arbitrary test condition. Our analysis suggests that a new blockage correction that accounts for rotation and better describes highly loaded turbines could be more effective and is an area deserving of future efforts.

Acknowledgments

This work was supported by the National Science Foundation Graduate Research Fellowship Program (grant number DGE-1256082) and the United States Department of Defense Naval Facilities Engineering Command. The authors acknowledge Dr. Martin Wosnik and Mr. John Ahern at the Center for Ocean Renewable Energy at the University of New Hampshire for hosting and facilitating experiments. The Alice C. Tyler Charitable Trust is acknowledged for supporting the experimental facilities at the University of Washington. Finally, Benjamin Strom and Katherine Van Ness are recognized for their significant contributions to the experimental set-ups used in this study. The funding organizations had no involvement in the study design or execution.

Data availability

The data and code that support this work are publicly accessible via ResearchWorks, the University of Washington's digital repository. The material may be accessed at http://hdl.handle.net/1773/43780.

Competing interests

The authors have no competing interests to declare.

References

[1] R. M. K. Wood, R. G. Harris, Some Notes on the Theory of an Airscrew Working in a Wind Channel, HMSO, London, 1921.

[2] H. Glauert, Airplane propellers, in: W. F. Durand (Ed.), Aerodynamic Theory: A General Review of Progress Under a Grant of the Guggenheim Fund for the Promotion of Aeronautics, volume 4, Springer, Berlin, 1935, pp. 169–360.

[3] C. Garrett, P. Cummins, The efficiency of a turbine in a tidal channel, J. Fluid Mech. 588 (2007) 243–251. doi:https://doi.org/10.1017/S0022112007007781.

[4] G. T. Houlsby, C. R. Vogel, The power available to tidal turbines in an open channel flow, Proc. Inst. Civ. Eng., Energy 170 (2017) 12–21. doi:https://doi.org/10.1680/jener.15.00035.

[5] T. Nishino, R. H. J. Willden, Effects of 3-D channel blockage and turbulent wake mixing on the limit of power extraction by tidal turbines, Int. J. Heat Fluid Flow 37 (2012) 123–135. doi:https://doi.org/10.1016/j.ijheatfluidflow.2012.05.002.

[6] C. A. Consul, R. H. J. Willden, S. C. McIntosh, Blockage effects on the hydrodynamic performance of a marine cross-flow turbine, Philos. Trans. - Royal Soc., Math. Phys. Eng. Sci. 371 (2013) 20120299. doi:https://doi.org/10.1098/rsta.2012.0299.

[7] A. Goude, O. Ågren, Simulations of a vertical axis turbine in a channel, Renew. Energy 63 (2014) 477–485. doi:https://doi.org/10.1016/j.renene.2013.09.038.

[8] N. Kolekar, A. Banerjee, Performance characterization and placement of a marine hydrokinetic turbine in a tidal channel under boundary proximity and blockage effects, Appl. Energy 148 (2015) 121–133. doi:https://doi.org/10.1016/j.apenergy.2015.03.052.

[9] J. Schluntz, R. H. J. Willden, The effect of blockage on tidal turbine rotor design and performance, Renew. Energy 81 (2015) 432–441. doi:https://doi.org/10.1016/j.renene.2015.02.050.

[10] H. Sarlak, T. Nishino, L. A. Martínez-Tossas, C. Meneveau, J. N. Sørensen, Assessment of blockage effects on the wake characteristics and power of wind turbines, Renew. Energy 93 (2016) 340–352. doi:https://doi.org/10.1016/j.renene.2016.01.101.

[11] T. Kinsey, G. Dumas, Impact of channel blockage on the performance of axial and cross-flow hydrokinetic turbines, Renew. Energy 103 (2017) 239–254. doi:https://doi.org/10.1016/j.renene.2016.11.021.

[12] A. S. Bahaj, A. F. Molland, J. R. Chaplin, W. M. J. Batten, Power and thrust measurements of marine current turbines under various hydrodynamic flow conditions in a cavitation tunnel and a towing tank, Renew. Energy 32 (2007) 407–426. doi:https://doi.org/10.1016/j.renene.2006.01.012.

[13] L. Battisti, L. Zanne, S. Dell'Anna, V. Dossena, G. Persico, B. Paradiso, Aerodynamic measurements of a vertical axis wind turbine in a large scale wind tunnel, J. Energy Resour. Technol. 133 (2011) 031201–1–031201–9. doi:https://doi.org/10.1115/1.4004360.

[14] A. H. Birjandi, E. L. Bibeau, V. Chatoorgoon, A. Kumar, Power measurement of hydrokinetic turbines with free-surface and blockage effect, Ocean Eng. 69 (2013) 9–17. doi:https://doi.org/10.1016/j.oceaneng.2013.05.023.

[15] S. McTavish, D. Feszty, F. Nitzsche, An experimental and computational assessment of blockage effects on wind turbine wake development, Wind Energy 17 (2014) 1515–1529. doi:https://doi.org/10.1002/we.1648.

[16] B. Gaurier, G. Germain, J. V. Facq, C. M. Johnstone, A. D. Grant, A. H. Day, E. Nixon, F. Di Felice, M. Costanzo, Tidal energy "Round Robin" tests comparisons between towing tank and circulating tank results, Int. J. Mar. Energy 12 (2015) 87–109. doi:https://doi.org/10.1016/j.ijome.2015.05.005.

[17] J. Ryi, W. Rhee, U. C. Hwang, J.-S. Choi, Blockage effect correction for a scaled wind turbine rotor by using wind tunnel test data, Renew. Energy 79 (2015) 227–235. doi:https://doi.org/10.1016/j.renene.2014.11.057.

[18] V. Dossena, G. Persico, B. Paradiso, L. Battisti, S. Dell'Anna, A. Brighenti, B. Enrico, An experimental study of the aerodynamics and performance of a vertical axis

wind turbine in a confined and unconfined environment, J. Energy Resour. Technol. 137 (2015) 051207–1–051207–12. doi:https://doi.org/10.1115/1.4030448.

[19] M. J. Barnsley, J. F. Wellicome, Final report on the 2nd phase of development and testing of a horizontal axis wind turbine test rig for the investigation of stall regulation aerodynamics, Technical Report E.5A/CON5103/1746, ETSU, 1990.

[20] R. Mikkelsen, J. N. Sørensen, Modelling of wind tunnel blockage, in: Global Windpower Conference, Paris, France, 2002.

[21] M. J. Werle, Wind turbine wall-blockage performance corrections, J. Propuls. Power 26 (2010) 1317–1321. doi:https://doi.org/10.2514/1.44602.

[22] G. T. Houlsby, S. Draper, M. L. G. Oldfield, Applicaton of Linear Momentum Actuator Disc Theory to Open Channel Flow, Technical Report OUEL 2296/08, University of Oxford, 2008.

[23] P. Bachant, M. Wosnik, Performance measurements of cylindrical- and spherical-helical cross-flow marine hydrokinetic turbines, with estimates of exergy efficiency, Renew. Energy 74 (2015) 318–325. doi:https://doi.org/10.1016/j.renene.2014.07.049.

[24] P. W. Galloway, L. E. Myers, A. S. Bahaj, Quantifying wave and yaw effects on a scale tidal stream turbine, Renew. Energy 63 (2014) 297–307. doi:https://doi.org/10.1016/j.renene.2013.09.030.

[25] A. Segalini, P. Inghels, Confinement effects in wind-turbine and propeller measurements, J. Fluid Mech. 756 (2014) 110–129. doi:https://doi.org/10.1017/jfm.2014.440.

[26] J. I. Whelan, J. M. R. Graham, J. Peiró, A free-surface and blockage correction for tidal turbines, J. Fluid Mech. 624 (2009) 281–291. doi:https://doi.org/10.1017/S0022112009005916.

[27] I. Ross, A. Altman, Wind tunnel blockage corrections: Review and application to savonius vertical-axis wind turbines, J. Wind Eng. Ind. Aerodynamics 99 (2011) 523–538. doi:https://doi.org/10.1016/j.jweia.2011.02.002.

[28] P. Stansby, T. Stallard, Fast optimisation of tidal stream turbine positions for power generation in small arrays with low blockage based on superposition of self-similar far-wake velocity deficit profiles, Renew. Energy 92 (2016) 366–375. doi:https://doi.org/10.1016/j.renene.2016.02.019.

[29] E. C. Maskell, A Theory of the Blockage Effects on Bluff Bodies and Stalled Wings in a Closed Wind Tunnel, HMSO, London, 1963.

[30] A. Pope, J. J. Harper, Low-Speed Wind Tunnel Testing, John Wiley and Sons, New York, 1966.

[31] L. P. Chamorro, R. E. A. Arndt, F. Sotiropoulos, Reynolds number dependence of turbulence statistics in the wake of wind turbines, Wind Energy 15 (2012) 733–742. doi:https://doi.org/10.1002/we.501.

[32] P. Bachant, M. Wosnik, Effects of Reynolds number on the energy conversion and near-wake dynamics of a high solidity vertical-axis cross-flow turbine, Energies 9 (2016). doi:https://doi.org/10.3390/en9020073.

[33] M. A. Miller, S. Duvvuri, I. Brownstein, M. Lee, J. O. Dabiri, M. Hultmark, Vertical-axis wind turbine experiments at full dynamic similarity, J. Fluid Mech. 844 (2018) 707–720. doi:https://doi.org/10.1017/jfm.2018.197.

[34] C. R. Vogel, G. T. Houlsby, R. H. J. Willden, Effect of free surface deformation on the extractable power of a finite width turbine array, Renew. Energy 88 (2016) 317–324. doi:https://doi.org/10.1016/j.renene.2015.11.050.

[35] B. Strom, N. Johnson, B. Polagye, Impact of blade mounting structures on cross-flow turbine performance, J. Renew. Sustain. Energy 10 (2018) 034504. doi:https://doi.org/10.1063/1.5025322.

[36] R. B. Barber, C. S. Hill, P. F. Babuska, R. Wiebe, A. Aliseda, M. R. Motley, Flume-scale testing of an adaptive pitch marine hydrokinetic turbine, Compos. Struct. 168 (2017) 465–473. doi:https://doi.org/10.1016/j.compstruct.2017.02.051.

[37] P. Bachant, M. Wosnik, Characterising the near-wake of a cross-flow turbine, J. Turbul. 16 (2015) 392–410. doi:https://doi.org/10.1080/14685248.2014.1001852.

[38] P. Mycek, B. Gaurier, G. Germain, G. Pinon, E. Rivoalen, Experimental study of the turbulence intensity effects on marine current turbines behaviour. part i: One single turbine, Renew. Energy 66 (2014) 729–746. doi:https://doi.org/10.1016/j.renene.2013.12.036.

[39] T. Blackmore, L. E. Myers, A. S. Bahaj, Effects of turbulence on tidal turbines: Implications to performance, blade loads, and condition monitoring, Int. J. Mar. Energy 14 (2016) 1–26. doi:https://doi.org/10.1016/j.ijome.2016.04.017.

[40] B. Polagye, B. Strom, H. Ross, D. Forbush, R. J. Cavagnaro, Comparison of cross-flow turbine performance under torque-regulated and speed-regulated control, 2019. In press.

[41] D. G. Goring, V. I. Nikora, Despiking acoustic Doppler velocimeter data, J. Hydraul. Eng. 128 (2002) 117–126. doi:https://doi.org/10.1061/(ASCE)0733-9429(2002)128:1(117).

[42] P. J. Rusello, A Practical Primer for Pulse Coherent Instruments, Technical Report TN-027, NortekUSA, 2009.

[43] M. Barnsley, J. Wellicome, Wind tunnel investigation of stall aerodynamics for a 1.0 m horizontal axis rotor, J. Wind Eng. Ind. Aerodynamics 39 (1992) 11–21. doi:https://doi.org/10.1016/0167-6105(92)90528-I.

[44] F. W. Lanchester, A contribution to the theory of propulsion and the screw propeller, J. Am. Soc. Naval Eng. 27 (1915) 509–510. doi:https://doi.org/10.1111/j.1559-3584.1915.tb00408.x.

[45] A. Betz, Das maximum der theoretisch möglichen ausnützung des windes durch windmotoren, Zeitschrift für dasgesamte Turbinenwesen 26 (1920) 307–309.

[46] H. Ross, B. Polagye, Supplementary material for "An experimental assessment of analytical blockage corrections for turbines", ResearchWorks Digital Repository, 2019. URL: `http://hdl.handle.net/1773/43780`.

[47] M. J. Werle, J. Presz, W. M., Shroud and ejector augmenters for subsonic propulsion and power systems, J. Propuls. Power 25 (2009) 228–236. doi:https://doi.org/10.2514/1.36042.

[48] H. Ross, B. Polagye, Experimental good practices for current turbines tested in transitional reynolds number regimes, 2019. Unpublished results.

[49] D. B. Araya, T. Colonius, J. O. Dabiri, Transition to bluff-body dynamics in the wake of vertical-axis wind turbines, J. Fluid Mech. 813 (2017) 346–381. doi:https://doi.org/10.1017/jfm.2016.862.